Spontaneous Symmetry Breaking in the Standard Model

Lorenzo Zavoli

June 9, 2025

Abstract

In this work, we examine the theoretical foundations of the Higgs mechanism within the Standard Model. Particularly, we focus on spontaneous symmetry breaking (SSB) and its role in generating the masses of gauge bosons and fermions, as well as their interactions with the Higgs boson. After discussing SSB in both discrete and continuous symmetries, we illustrate how it leads to the Higgs mechanism in the electroweak sector. Finally, we review experimental results from the CMS collaboration on the measurement of the Higgs boson mass and, more specifically, on the tests of its couplings to other Standard Model particles. These results show no significant deviations from the theoretical predictions of the Standard Model.

1 Introduction

The Higgs mechanism is a key component of the Standard Model, providing a theoretical framework for understanding how elementary particles acquire mass through their interactions with the Higgs field. Central to this mechanism is the concept of spontaneous symmetry breaking, a phenomenon in which the ground state of a system does not respect the symmetries of the corresponding Lagrangian.
In Sec. 2, we introduce the general idea of spontaneous symmetry breaking. In Sec. 3, we examine the breaking of discrete symmetries, while in Sec. 4 the case of continuous symmetries. Then, in Sec. 5, we explore the SSB of a gauge symmetry. First, we study the easier case of the Abelian Higgs model, consisting of the SSB of a local U(1) symmetry. Subsequently, we move to the general case of Higgs Mechanism for the Electroweak Theory, and its role in giving mass to the W and Z bosons, as well as to charged leptons. Finally, in Sec. 6, we review some experimental tests of the compatibility of the Higgs couplings with the Standard Model predictions. These include the measurement of the ratio of the couplings to W and Z bosons, the compatibility of couplings to vector bosons and fermions, and possible asymmetries or scaling deviations in the couplings. The consistency of these results with theoretical expectations supports the robustness of the Higgs mechanism within the Standard Model framework.

2 The idea of spontaneous symmetry breaking

In nature, there seem to exist exact conservation laws, such as conservation of energy and momentum, or of angular momentum. In Lagrangian field theory, a symmetry is said to be

exact if it leaves the Lagrangian invariant,

$$\delta\mathcal{L} = 0, \tag{1}$$

and the unique physical vacuum is invariant under the symmetry transformations. In such cases, Noether's theorem ensures the existence of exact conservation laws. However, many of the useful internal symmetries in particle physics, such as the isospin or the conservation of strangeness and charm, hold only approximately.
In particular, there are different kinds of symmetry breaking. In explicit symmetry breaking, the Lagrangian is not invariant under the symmetry transformations. It is useful to express the Lagrangian as

$$\mathcal{L} = \mathcal{L}_{sym} + \epsilon\ \mathcal{L}_{breaking}, \tag{2}$$

if the symmetry-breaking term $\mathcal{L}_{breaking}$ is small, in some sense, and can be treated as a perturbation of the symmetric interaction $\mathcal{L}_{sym}$. In this case of small violation of the symmetry, approximate conservation laws may still arise.
In contrast, a symmetry is said to be spontaneously broken when the Lagrangian $\mathcal{L}$ is exactly invariant under some symmetry, so that (1) holds, but it has a degenerate set of vacuum states that are not invariant under the symmetry. Thus, each vacuum breaks the symmetry, even though the Lagrangian respect it. This leads to exact conservation laws, but the symmetry is hidden in observable quantities.
An example of symmetry breaking is provided by an infinite ferromagnet. Above the Curie temperature $\mathrm{T_C}$, the ferromagnet is in the paramagnetic phase. Thermal fluctuations dominate over the dipole-dipole interactions, and the orientation of individual spins is random. In absence of an external field, the system exhibits an unbroken SO(3) symmetry, the spontaneous magnetization vanishes ($\langle\vec{M}\rangle = 0$), and there is no preferred direction in space. By imposing an external magnetic field that biases the alignment of spins in the material, the SO(3) symmetry is thus broken down to an SO(2) symmetry of rotations about the external field direction. The full symmetry is restored when the external field is turned off.
Below $\mathrm{T_C}$ the system is in the ferromagnetic phase. Even in the absence of an impressed field, the nearest-neighbor interactions favors the parallel alignment of spins, and a non-zero spontaneous magnetization appears: $\langle\vec{M}\rangle \neq 0$. In these circumstances, the SO(3) symmetry is said to be spontaneously broken down to SO(2). The direction of the spontaneous magnetization is random, resulting in an infinitely degenerate set of ground states. The measurable properties of the infinite ferromagnet remain independent of the aleatory choice of magnetization direction. These residual invariances are manifestations of the original SO(3) symmetry, which is thus said to be hidden in the physical vacuum.

3 Spontaneous breaking of discrete symmetries

Let us consider a real scalar field ϕ, and its associated Lagrangian

$$\mathcal{L} = \frac{1}{2}(\partial_\mu\phi)(\partial^\mu\phi) - V(\phi), \tag{3}$$

with a self-interacting potential $V(\phi)$ such that

$$V(\phi) = \frac{1}{2}\mu^2\phi^2 + \frac{1}{4}\,|\lambda|\,\phi^4. \tag{4}$$

The potential $V(\phi)$ is symmetric under a parity transformation:

$$V(\phi) = V(-\phi). \tag{5}$$

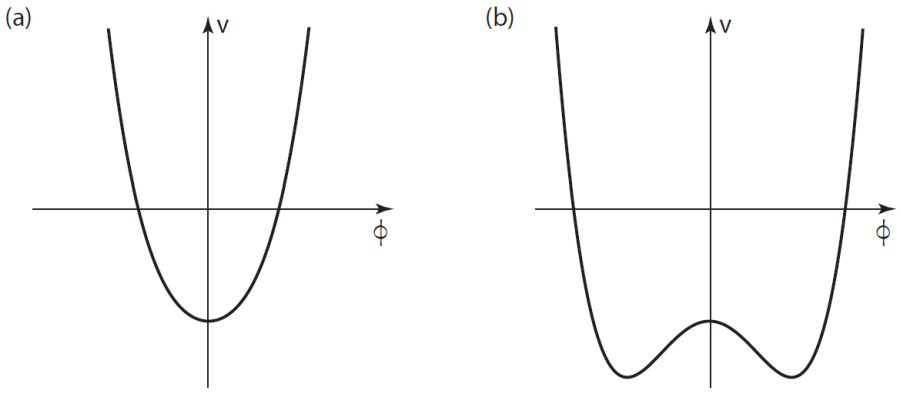

Figure 1: (left) Single-well potential with a unique minimum at $\phi = 0$; (right) double-well potential with a degenerate vacuum, corresponding to a spontaneously broken symmetry [1]

Considering the Hamiltonian formalism, the Hamiltonian density is given by

$$\mathcal{H} = \pi\dot{\phi} - \mathcal{L}, \tag{6}$$

which, in this case, becomes

$$\mathcal{H} = \frac{1}{2}\left[(\partial_0\phi)^2 + (\nabla\phi)^2\right] + V(\phi). \tag{7}$$

The state of lowest energy is characterized by a constant value of the field ϕ, which we denote as $\langle\phi\rangle_0$. If the parameter μ^2 is positive, the minimum of the potential is at $\langle\phi\rangle_0 = 0$, as shown in Figure 1 (left).
If $\mu^2 < 0$, the system exhibits a spontaneously broken symmetry. The potential, shown in Figure 1 (right), has minima at

$$\langle\phi\rangle_0 = \pm\sqrt{\frac{-\mu^2}{|\lambda|}} \equiv \pm v, \tag{8}$$

where v is called vacuum expectation value. These correspond to two degenerate ground states, either of which may be chosen as the vacuum. Although the Lagrangian is invariant under the parity transformation $\phi \to -\phi$, the choice of a specific vacuum spontaneously breaks this symmetry. Nevertheless, due to the underlying symmetry of the Lagrangian, the physical predictions must be independent of this choice. Let us choose $\phi_0 = +v$. We define a shifted field

$$\eta \equiv \phi - \phi_0 = \phi - v, \tag{9}$$

so that the vacuum state corresponds to

$$\langle\eta\rangle_0 = 0. \tag{10}$$

In terms of the shifted field, the Lagrangian becomes

$$\mathcal{L} = \frac{1}{2}(\partial_\mu\eta)(\partial^\mu\eta) - |\mu|^2\left(\frac{\eta^4}{4v^2} + \frac{\eta^3}{v} + \eta^2 - \frac{v^2}{4}\right), \tag{11}$$

which has no manifest symmetry properties with respect to the shifted field η. For small oscillations about the vacuum, we have

$$\mathcal{L}_{\text{so}} \propto \frac{1}{2}\left[(\partial_\mu\eta)(\partial^\mu\eta) - 2|\mu|^2\eta^2\right], \tag{12}$$

which describes the oscillation of a particle with mass m_η:

$$m_\eta^2 = -2\mu^2. \tag{13}$$

This example illustrates the case of a spontaneously broken discrete symmetry. We are now ready to examine the case of a continuous symmetry.

4 Spontaneous breaking of continuous symmetries

Let us consider the Lagrangian of two scalar fields ϕ_1 and ϕ_2:

$$\mathcal{L} = \frac{1}{2}\left[(\partial_\mu\phi_1)(\partial^\mu\phi_1) + (\partial_\mu\phi_2)(\partial^\mu\phi_2)\right] - V(\phi_1^2 + \phi_2^2). \tag{14}$$

The Lagrangian is invariant under the group SO(2) of rotations in the plane:

$$\boldsymbol{\phi} \equiv \begin{pmatrix}\phi_1\\ \phi_2\end{pmatrix} \to \begin{pmatrix}\cos\theta & \sin\theta\\ -\sin\theta & \cos\theta\end{pmatrix}\begin{pmatrix}\phi_1\\ \phi_2\end{pmatrix}. \tag{15}$$

As we did before in the case of a discrete symmetry (Sec. 3), we consider the effective potential

$$V(\phi^2) = \frac{1}{2}\mu^2\phi^2 + \frac{1}{4}|\lambda|(\phi^2)^2, \tag{16}$$

where $\phi^2 = \phi_1^2 + \phi_2^2$, and distinguish two cases.
A positive value of the parameter $\mu^2 > 0$ corresponds to the ordinary case of unbroken symmetry, illustrated by the potential in Figure 2 (left). The potential has a unique minimum, which corresponds to the vacuum state

$$\langle\boldsymbol{\phi}\rangle_0 = \begin{pmatrix}0\\ 0\end{pmatrix}. \tag{17}$$

For small oscillations around the vacuum, the Lagrangian becomes:

$$\mathcal{L}_{\rm so} = \frac{1}{2}\left[(\partial_\mu\phi_1)^2 - \mu^2\phi_1^2\right] + \frac{1}{2}\left[(\partial_\mu\phi_2)^2 - \mu^2\phi_2^2\right]. \tag{18}$$

This is the same as the Lagrangian for a pair of real scalar particles, each with mass μ. Thus, the SO(2) symmetry is still manifest, and the degenerate multiplet structure of the free theory is preserved.
In contrast, the choice $\mu^2 < 0$ leads to a spontaneously broken symmetry. In this case, the potential takes the form shown in Figure 2 (right), without a unique minimum. Instead, the minima of the potential now occurs for

$$\langle\phi^2\rangle_0 = \frac{-\mu^2}{|\lambda|} = v^2, \tag{19}$$

which corresponds to a continuum of distinct vacuum states, degenerate in energy. The degeneracy arises from the SO(2) symmetry of the Lagrangian: the set of vacuum states is invariant under SO(2) transformations. However, choosing one state as the vacuum selects a preferred direction in the (ϕ_1, ϕ_2) internal symmetry space, breaking the SO(2) symmetry spontaneously.
Now, we can proceed as we did in the previous case of a discrete symmetry. Let us select as the physical vacuum state the configuration

$$\langle\boldsymbol{\phi}\rangle_0 = \begin{pmatrix}v\\ 0\end{pmatrix}, \tag{20}$$

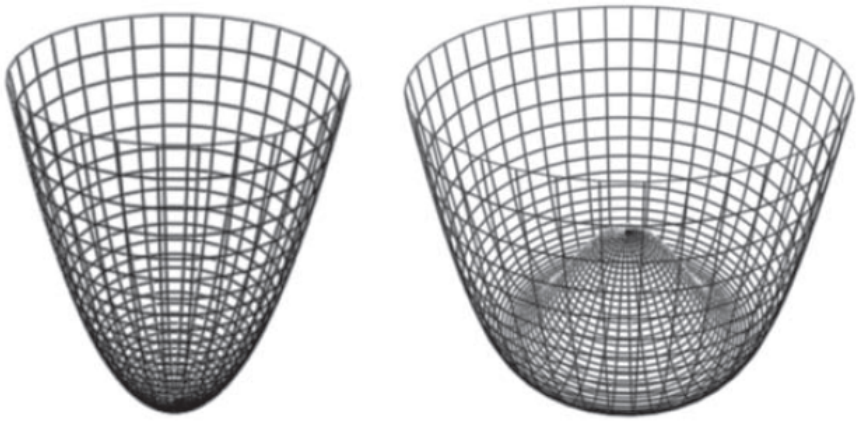

Figure 2: (left) Potential with a unique minimum at $\phi_1 = \phi_2 = 0$; (right) Potential with a degenerate vacuum at $\phi_1^2 + \phi_2^2 \neq 0$; selecting a vacuum spontaneously breaks the rotation symmetry [1].

and expanding about the vacuum configuration by defining the shifted field

$$\boldsymbol{\phi}' \equiv \boldsymbol{\phi} - \langle \boldsymbol{\phi} \rangle_0 \equiv \begin{pmatrix} \eta \\ \zeta \end{pmatrix}, \tag{21}$$

we obtain the Lagrangian for small oscillations:

$$\mathcal{L}_{\text{so}} \propto \frac{1}{2}\left[(\partial_\mu \eta)(\partial^\mu \eta) + 2\mu^2 \eta^2\right] + \frac{1}{2}\left[(\partial_\mu \zeta)(\partial^\mu \zeta)\right]. \tag{22}$$

The η-particle, associated with radial oscillations, has a mass

$$m_\eta^2 = -2\mu^2 \tag{23}$$

just as we found for the particle in the case of a spontaneously broken parity invariance. The ξ-particle, however, is massless. The mass of the η-particle may be viewed as a consequence of the restoring force of the potential against radial oscillations. In contrast, the masslessness of the ξ-particle arises from the SO(2) invariance of the Lagrangian, which implies the absence of a restoring force against angular oscillations. These massless particles are known as Nambu–Goldstone bosons, and their existence is explained by the so-called *Goldstone theorem*: if a continuous global symmetry of $\mathcal{L}$ is not a symmetry of the physical vacuum, then exists one Goldstone boson for each generator of the broken symmetry [2].

5 Spontaneous breaking of a gauge symmetry

In the previous sections, we have discussed spontaneous symmetry breaking in systems with global symmetries, both discrete and continuous. We now turn to the more physically significant case in which the spontaneously broken symmetry is a local gauge symmetry.

Unlike global symmetries, the spontaneous breaking of a gauge symmetry does not lead to massless Nambu–Goldstone bosons. In this case, the scalar degrees of freedom that would appear as massless particles if the symmetry were global, are instead "absorbed" by the gauge field. This absorption provides the gauge bosons with an additional longitudinal polarization component, effectively giving them mass through a process known as the Higgs mechanism.

This phenomenon is first illustrated through the Abelian Higgs model, which serves as a simple example. We then move on to the Electroweak Theory, where spontaneous gauge symmetry breaking provides mass to the weak vector bosons while preserving gauge invariance.

5.1 Abelian Higgs model

Let us consider the Lagrangian

$$\mathcal{L} = |D_\mu \phi|^2 - \mu^2 |\phi|^2 - |\lambda|(\phi^* \phi)^2 - \frac{1}{4} F_{\mu\nu} F^{\mu\nu}, \tag{24}$$

where

$$\phi = \frac{1}{\sqrt{2}}(\phi_1 + i\phi_2) \tag{25}$$

is a complex scalar field, and,

$$D_\mu \equiv \partial_\mu + iqa_\mu, \tag{26}$$
$$F_{\mu\nu} \equiv \partial_\nu a_\mu - \partial_\mu a_\nu, \tag{27}$$

are respectively the covariant derivative and the energy-momentum tensor. The Lagrangian is invariant under $U(1)$ rotations

$$\phi \to \phi' = e^{i\theta}\phi, \tag{28}$$

and under the local gauge transformations

$$\phi(x) \to \phi'(x) = e^{iq\alpha(x)}\phi(x), \tag{29}$$
$$a_\mu(x) \to a'_\mu(x) = a_\mu(x) - \partial_\mu \alpha(x). \tag{30}$$

As the previous case, the behavior of the effective potential depends on the sign of the parameter μ^2, leading to two physically distinct scenarios.
When $\mu^2 > 0$, the potential has a single absolute minimum at $\phi = 0$, and the exact symmetry of the Lagrangian is preserved. The particle spectrum coincides with that of ordinary QED: there is a massless photon a_μ, and two complex scalar fields, ϕ and ϕ^*, with mass μ. When $\mu^2 < 0$, the potential has a continuum of absolute minima, corresponding to a continuum of degenerate vacua, at

$$\langle |\phi|^2 \rangle_0 = \frac{-\mu^2}{2|\lambda|} \equiv \frac{v^2}{2}. \tag{31}$$

Although the Lagrangian remains symmetric, the choice of a specific vacuum spontaneously breaks the symmetry. To analyze the particle spectrum in the symmetry-broken phase, we shift the field in order to express the Lagrangian in terms of fluctuations around the chosen vacuum. Since all the vacua are physically equivalent, we can choose without loss of generality:

$$\langle \phi \rangle_0 = \frac{v}{\sqrt{2}}, \quad v > 0. \tag{32}$$

We define the shifted field

$$\tilde{\phi} = \phi - \langle \phi \rangle_0, \tag{33}$$

which we parameterize as

$$\tilde{\phi} = \frac{1}{\sqrt{2}} e^{i\zeta/v}(v + \eta) \approx \frac{1}{\sqrt{2}}(v + \eta + i\zeta). \tag{34}$$

Then, the Lagrangian for small oscillations becomes

$$\mathcal{L}_{\text{so}} \propto \frac{1}{2}(\partial_\mu \eta)(\partial^\mu \eta) + \mu^2 \eta^2 + \frac{1}{2}(\partial_\mu \zeta)(\partial^\mu \zeta) - \frac{1}{4} F_{\mu\nu} F^{\mu\nu} + qva^\mu \partial_\mu \zeta + \frac{q^2 v^2}{2} a^\mu a_\mu, \tag{35}$$

and we observe that:

- The η field has mass squared $-2\mu^2 > 0$, as expected from the Goldstone mechanism,
- The gauge field a_μ appears to have acquired a mass, but is mixed in the $qva^\mu\partial_\mu\zeta$ term with the massless field ζ.

Rewriting the terms which contain a_μ and ζ as

$$\frac{q^2v^2}{2}\left(a_\mu + \frac{1}{qv}\partial_\mu\zeta\right)^2, \tag{36}$$

let us consider the gauge transformation

$$a_\mu \to a'_\mu = a_\mu + \frac{1}{qv}\partial_\mu\zeta, \tag{37}$$

which corresponds to the phase rotation:

$$\tilde{\phi} \to \tilde{\phi}' = e^{-i\zeta(x)/v}\tilde{\phi}(x) = \frac{v+\eta}{\sqrt{2}}. \tag{38}$$

This gauge choice is called unitary gauge (or U-gauge). In the unitary gauge, the Lagrangian for small oscillations becomes

$$\mathcal{L}_{\text{so}} \propto \frac{1}{2}(\partial_\mu\eta)(\partial^\mu\eta) + \mu^2\eta^2 - \frac{1}{4}F_{\mu\nu}F^{\mu\nu} + \frac{q^2v^2}{2}a'^\mu a'_\mu. \tag{39}$$

With this gauge choice, the particle spectrum consists in:

- A scalar field η, with mass $m_\eta^2 = -2\mu^2 = 2\lambda v^2$,
- A massive vector field a'_μ, with mass $m_a = qv$,
- No ζ field.

The ζ particle has disappeared from the Lagrangian: what was formerly the ζ field has become the longitudinal component of the massive vector field a'_μ. Before spontaneous symmetry breaking, the theory had four particle degrees of freedom, two scalars ϕ and ϕ^*, and two helicity states of the massless gauge field a_μ. After symmetry breaking, there is one scalar particle η, and three helicity states of the massive vector field a'_μ. The massless Nambu–Goldstone boson has been absorbed by the massless photon, which has become a massive vector boson. The remaining massive scalar (η) is known as the Higgs boson.
In the next section, we will see how this mechanism, known as Higgs Mechanism, allows to provide mass to weak vector bosons without breaking gauge invariance.

5.2 The Electroweak Theory of Leptons and the Higgs Mechanism

Consider now the $\mathrm{SU(2)_L} \otimes \mathrm{U(1)_Y}$ Electroweak Theory in its purely leptonic form. In particular, let us consider only the first generation of lepton, with the electron and its associated neutrino. These form a left-handed weak isospin doublet

$$L \equiv \begin{pmatrix}\nu_e \\ e\end{pmatrix}_L, \tag{40}$$

where the left-handed projections are defined as

$$\nu_L = \frac{1}{2}(1-\gamma^5)\nu, \quad e_L = \frac{1}{2}(1-\gamma^5)e. \tag{41}$$

In the Standard Model, neutrinos are assumed to be massless. As a result, the right-handed neutrino state does not exist in the theory. We then define only one right-handed lepton,

$$R = e_R = \frac{1}{2}(1+\gamma^5)e, \tag{42}$$

which is a weak isospin singlet.
To incorporate electromagnetism within the electroweak framework, we introduce the weak hypercharge Y. Imposing the validity of the Gell-Mann–Nishijima relation,

$$Q = T_3 + \frac{1}{2}Y, \tag{43}$$

allows us to determine the appropriate hypercharge assignments for the fields. In particular, we find:

$$Y_L = -1, \quad Y_R = -2. \tag{44}$$

By construction, the weak isospin projection T_3 and the weak hypercharge Y are commuting observables:

$$[T_3, Y] = 0. \tag{45}$$

We now define the gauge group of the theory as $SU(2)_L \otimes U(1)_Y$. The associated gauge bosons are $b^1_\mu, b^2_\mu, b^3_\mu$ for $SU(2)_L$, and a_μ for $U(1)_Y$.
The Lagrangian of the theory is

$$\mathcal{L} = \mathcal{L}_{\text{gauge}} + \mathcal{L}_{\text{leptons}}. \tag{46}$$

The $\mathcal{L}_{\text{gauge}}$ term represents the kinetic term for the gauge fields,

$$\mathcal{L}_{\text{gauge}} = -\frac{1}{4}F^l_{\mu\nu}F^{l\mu\nu} - \frac{1}{4}f_{\mu\nu}f^{\mu\nu}, \tag{47}$$

where the field-strength tensor for the $\mathrm{SU(2)_L}$ gauge fields is defined as

$$F^l_{\mu\nu} = \partial_\mu b^l_\nu - \partial_\nu b^l_\mu + g\varepsilon^{ljk}b^j_\mu b^k_\nu, \tag{48}$$

and $f_{\mu\nu}$ is the $\mathrm{U(1)_Y}$ field-strength tensor, which is the same as the one defined in Eq. (27).
The $\mathcal{L}_{\text{leptons}}$ term represents the matter term,

$$\mathcal{L}_{\text{leptons}} = \bar{R}i\gamma^\mu\left(\partial_\mu + i\frac{g'}{2}a_\mu Y\right)R + \bar{L}i\gamma^\mu\left(\partial_\mu + i\frac{g'}{2}a_\mu Y + i\frac{g}{2}\boldsymbol{\tau}\cdot\mathbf{b}_\mu\right)L, \tag{49}$$

where g is the coupling of the weak isospin group $\mathrm{SU(2)_L}$ and $g'/2$ the one for the weak hypercharge group $\mathrm{U(1)_Y}$.
The weak and electromagnetic theory as presented has two main problems. First, it predicts the existence of four massless gauge bosons (b^1, b^2, b^3, and a), whereas experimentally only one massless gauge boson is observed, the photon. In addition, the electron remains massless in this framework, since the $-m_e\bar{e}e$ mass term of QED is absent. This occurs because the left-handed and right-handed components of the electron transform differently under the gauge group $\mathrm{SU(2)_L \otimes U(1)_Y}$. Thus, the explicit fermion mass term

$$\bar{e}e = \frac{1}{2}\bar{e}(1-\gamma^5)e + \frac{1}{2}\bar{e}(1+\gamma^5)e = \bar{e}_R e_L + \bar{e}_L e_R, \tag{50}$$

would brake the $\mathrm{SU(2)_L \otimes U(1)_Y}$ gauge invariance. Therefore, the introduction of an explicit fermion mass term is forbidden by gauge symmetry.

To overcome this issue, we introduce the complex scalar doublet

$$\phi \equiv \begin{pmatrix} \phi^+ \\ \phi^0 \end{pmatrix}, \tag{51}$$

that transforms as an $\mathrm{SU(2)_L}$ doublet and must, therefore, have weak hypercharge

$$Y_\phi = +1 \tag{52}$$

by the Gell-Mann–Nishijima relation (43).
We add to the Lagrangian a scalar field term given by

$$\mathcal{L}_{\text{scalar}} = (D_\mu \phi)^\dagger (D^\mu \phi) - V(\phi^\dagger \phi), \tag{53}$$

where the covariant derivative is defined as

$$D_\mu = \partial_\mu + i\frac{g'}{2} a_\mu Y + i\frac{g}{2} \boldsymbol{\tau} \cdot \mathbf{b}_\mu, \tag{54}$$

and the scalar potential takes the usual self-interaction form

$$V(\phi^\dagger \phi) = \mu^2 (\phi^\dagger \phi) + |\lambda| (\phi^\dagger \phi)^2. \tag{55}$$

Furthermore, we introduce the Yukawa interaction term, coupling the scalar field to the fermions:

$$\mathcal{L}_{\text{Yukawa}} = -\lambda_e \left[\bar{R}_e (\phi^\dagger L_e) + (\bar{L}_e \phi) R_e \right], \tag{56}$$

which is invariant under the local gauge group $\mathrm{SU(2)_L} \otimes \mathrm{U(1)_Y}$. The coupling constant λ_e is called Yukawa coupling.
Assuming $\mu^2 < 0$, spontaneous symmetry breaking occurs, and we can choose the vacuum expectation value as

$$\langle \phi \rangle_0 = \begin{pmatrix} 0 \\ \frac{v}{\sqrt{2}} \end{pmatrix}. \tag{57}$$

It can be easily shown that this state brakes both $\mathrm{SU(2)_L}$ and $\mathrm{U(1)_Y}$ symmetries. Let us recall that there is one Goldstone boson for each generator of the gauge symmetry that does not leave the vacuum invariant. The vacuum is left invariant by a generator G if

$$e^{i\alpha G} \langle \phi \rangle_0 = \langle \phi \rangle_0. \tag{58}$$

For an infinitesimal transformation, this condition becomes

$$(1 + i\alpha G) \langle \phi \rangle_0 = \langle \phi \rangle_0, \tag{59}$$

so that the condition for G to leave the vacuum invariant is simply

$$G \langle \phi \rangle_0 = 0. \tag{60}$$

Generators that satisfy this condition correspond to unbroken symmetries, whereas those that do not leave the vacuum invariant correspond to broken symmetries and give rise to Goldstone bosons.
We can now check that condition for the $\mathrm{SU(2)_L} \otimes \mathrm{U(1)_Y}$ generators:

$$\tau_1 \langle \phi \rangle_0 = \begin{pmatrix} 0 & 1 \\ 1 & 0 \end{pmatrix} \begin{pmatrix} 0 \\ v/\sqrt{2} \end{pmatrix} = \begin{pmatrix} v/\sqrt{2} \\ 0 \end{pmatrix} \neq 0, \tag{61}$$

$$\tau_2\langle\phi\rangle_0 = \begin{pmatrix} 0 & -i \\ i & 0 \end{pmatrix}\begin{pmatrix} 0 \\ v/\sqrt{2} \end{pmatrix} = \begin{pmatrix} -iv/\sqrt{2} \\ 0 \end{pmatrix} \neq 0, \tag{62}$$

$$\tau_3\langle\phi\rangle_0 = \begin{pmatrix} 1 & 0 \\ 0 & -1 \end{pmatrix}\begin{pmatrix} 0 \\ v/\sqrt{2} \end{pmatrix} = \begin{pmatrix} 0 \\ -v/\sqrt{2} \end{pmatrix} \neq 0, \tag{63}$$

$$Y\langle\phi\rangle_0 = Y_\phi\langle\phi\rangle_0 = +1\begin{pmatrix} 0 \\ v/\sqrt{2} \end{pmatrix} = \begin{pmatrix} 0 \\ v/\sqrt{2} \end{pmatrix} \neq 0, \tag{64}$$

showing that both symmetries are broken.
However, considering the electric charge operator (43), we find that

$$Q\langle\phi\rangle_0 = (T_3 + \frac{1}{2}Y)\langle\phi\rangle_0 = \frac{1}{2}\begin{pmatrix} Y_\phi + 1 & 0 \\ 0 & Y_\phi - 1 \end{pmatrix}\begin{pmatrix} 0 \\ v/\sqrt{2} \end{pmatrix} = \begin{pmatrix} 0 \\ 0 \end{pmatrix}. \tag{65}$$

This shows that the vacuum is left invariant by the generator of electric charge Q, meaning that the subgroup $\mathrm{U(1)_{EM}}$ remains unbroken after spontaneous symmetry breaking of the gauge group $\mathrm{SU(2)_L} \otimes \mathrm{U(1)_Y}$. Hence, the spontaneous symmetry breaking pattern in the electroweak theory is:

$$SU(2)_L \otimes U(1)_Y \to U(1)_{EM}. \tag{66}$$

Therefore, three of the four original gauge bosons acquire mass by absorbing the corresponding Goldstone boson, becoming the massive $W^\pm$ and Z^0 bosons. The remaining massless gauge boson corresponds to the unbroken $U(1)_{EM}$ and is identified with the physical photon.

We now expand the Higgs field around the vacuum in the U-gauge as

$$\phi(x) = \begin{pmatrix} 0 \\ \frac{v+\eta(x)}{\sqrt{2}} \end{pmatrix}, \tag{67}$$

and the kinetic term inside the scalar Lagrangian becomes

$$\begin{aligned}(D_\mu\phi)^\dagger(D^\mu\phi) = &\frac{1}{2}(\partial_\mu\eta)(\partial^\mu\eta) + \frac{1}{8}g^2|b^1_\mu - ib^2_\mu|^2(v+\eta)^2 \\ &+ \frac{1}{8}(g'a_\mu - gb^3_\mu)^2(v+\eta)^2.\end{aligned} \tag{68}$$

Defining the charged gauge fileds as

$$W^\pm_\mu = \frac{b^1_\mu \mp ib^2_\mu}{\sqrt{2}}, \tag{69}$$

we obtain a mass term

$$\frac{g^2v^2}{4}(|W^+_\mu|^2 + |W^-_\mu|^2) \tag{70}$$

for this fields, where the charged intermediate boson masses are

$$M_{W^\pm} = \frac{gv}{2}. \tag{71}$$

Defining the orthogonal combinations

$$Z_\mu = \frac{-g'a_\mu + g\,b^3_\mu}{\sqrt{g^2 + g'^2}} \tag{72}$$

and

$$A_\mu = \frac{g a_\mu + g' b^3_\mu}{\sqrt{g^2 + g'^2}} \tag{73}$$

of the generators a_μ and b^3_μ, we find that the neutral intermediate boson Z^0 has acquired a mass

$$M_Z = \frac{\sqrt{g^2 + g'^2}\, v}{2} = M_W \sqrt{1 + g'^2/g^2}, \tag{74}$$

while the field A_μ remains a massless gauge boson, corresponding to the surviving $\mathrm{U(1)_{EM}}$ symmetry.
As previously discussed in Sec. 4, from the scalar Lagrangian, the degree of freedom η, corresponding to fluctuations around the vacuum in the radial direction, acquires a mass

$$m_H^2 = -2\mu^2. \tag{75}$$

This massive particle corresponds to the physical Higgs boson H.
Finally, defining the weak mixing angle θ_W as

$$g' = g \tan\theta_W, \tag{76}$$

we can parametrize the mixing of the neutral gauge bosons as

$$Z_\mu = -a_\mu \sin\theta_W + b^3_\mu \cos\theta_W, \tag{77}$$

$$A_\mu = a_\mu \cos\theta_W + b^3_\mu \sin\theta_W. \tag{78}$$

From the relation (74), substituting the definition of the weak mixing angle, we find that

$$M_Z = M_W \sqrt{1 + \frac{sin^2\theta_W}{cos^2\theta_W}} = \frac{M_W}{cos\theta_W}. \tag{79}$$

This leads to a prediction of the standard model for the ratio of the $W^\pm$ and Z bosons masses:

$$\frac{M_W}{M_Z} = cos\theta_W. \tag{80}$$

Thus, by measuring the value of the gauge boson masses, we can infer the value of the weak mixing angle θ_W, obtaining

$$sin(\theta_W) = 1 - \left(\frac{M_W}{M_Z}\right)^2 \approx 0.223. \tag{81}$$

5.2.1 Higgs couplings with the gauge bosons

From the kinetic term (68) we get also the interaction terms between the gauge bosons and the Higgs boson:

$$\frac{1}{4} g_W^2 W^-_\mu W^{+\mu} (v + \eta)^2 = M_W^2 W^-_\mu W^{+\mu} + 2\frac{M_W^2}{v} W^-_\mu W^{+\mu}\eta + \frac{M_W^2}{v^2} W^-_\mu W^{+\mu}\eta^2. \tag{82}$$

Along with the already seen W boson mass term, the other two terms give rise to triple coupling ($WW\eta$) and quartic coupling ($WW\eta\eta$), both proportional to the mass M_W and the vacuum expectation value v. Analogously, for the Z^0 boson we get

$$\frac{1}{8}(g^2 + g'^2) Z_\mu Z^\mu (v + \eta)^2 = \frac{1}{2} M_Z^2 Z_\mu Z^\mu + \frac{M_Z^2}{v} Z_\mu Z^\mu \eta + \frac{1}{2}\frac{M_Z^2}{v^2} Z_\mu Z^\mu \eta^2, \tag{83}$$

with triple coupling ($ZZ\eta$) and quartic coupling ($ZZ\eta\eta$), both proportional to the mass M_Z and the vacuum expectation value v. The Higgs coupling with the gauge bosons $W^{\pm}$ and Z^0 are reported in Figure 3.

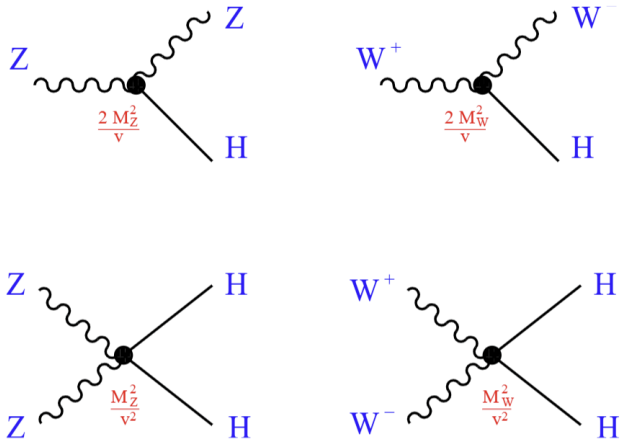

Figure 3: Higgs couplings with the gauge bosons $W^{\pm}$ and Z^0 [3].

5.2.2 Leptons

Before spontaneous symmetry breaking, a fermionic mass term is not allowed, as it would break the gauge symmetry. However, the previously introduced Yukawa term, in the unitary gauge, becomes

$$\begin{aligned}\mathcal{L}_{\text{Yukawa}} &= -\lambda_e \frac{(v+\eta)}{\sqrt{2}} \left(\bar{e}_R e_L + \bar{e}_L e_R\right) \\ &= -\frac{\lambda_e v}{\sqrt{2}}\, \bar{e}e - \frac{\lambda_e \eta}{\sqrt{2}}\, \bar{e}e. \end{aligned} \tag{84}$$

It turns out that the electron has acquired a mass

$$m_e = \frac{\lambda_e v}{\sqrt{2}} \tag{85}$$

by the first term, while the second term gives rise to the electron (or, more in general, charged lepton) interaction with the Higgs boson, which depends on its mass m_e and v (Figure 4). It can be observed that there is no mass term for neutrino, and even no coupling term with the Higgs field, which couples only with the lower component of the $\mathrm{SU(2)_L}$ doublet.
It is important to say that the the Yukawa couplings are not predicted by the theory, since the Yukawa is not a gauge interaction, but can be chosen as before to correspond to the fermion masses.

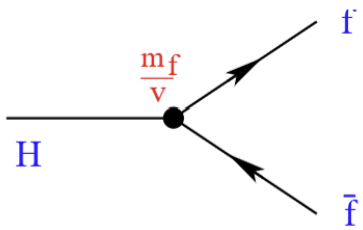

Figure 4: Fermionic coupling of the Higgs boson [3].

The interactions among the gauge bosons and leptons can be read from the matter term (49) in the Lagrangian. The coupling $\frac{g}{2}\boldsymbol{\tau}\cdot\mathbf{b}_\mu$ can be expanded in terms of the physical gauge bosons $W^\pm_\mu$, Z_μ and A_μ as

$$\begin{aligned}\frac{g}{2}\boldsymbol{\tau}\cdot\mathbf{b}_\mu &= \frac{g}{2}\begin{pmatrix} b^3_\mu & b^1_\mu - ib^2_\mu \\ b^1_\mu + ib^2_\mu & -b^3_\mu \end{pmatrix} \\ &= \frac{g}{2}\begin{pmatrix} \cos\theta_W Z_\mu + \sin\theta_W A_\mu & \sqrt{2}W^+_\mu \\ \sqrt{2}W^-_\mu & -\cos\theta_W Z_\mu - \sin\theta_W A_\mu \end{pmatrix}. \end{aligned} \tag{86}$$

Considering the off-diagonal terms, we obtain the charged current interactions mediated by the charged gauge bosons

$$\begin{aligned}\mathcal{L}_{CC} &= -\frac{g}{\sqrt{2}}\left(\bar\nu_L\gamma^\mu e_L W^+_\mu + \bar e_L\gamma^\mu\nu_L W^-_\mu\right) \\ &= -\frac{g}{2\sqrt{2}}\left(\bar\nu\gamma^\mu(1-\gamma^5)e\,W^+_\mu + \bar e\gamma^\mu(1-\gamma^5)\nu\,W^-_\mu\right). \end{aligned} \tag{87}$$

The electroweak theory matches the low-energy phenomenology of the weak interaction, provided that we identify the coupling constants as

$$\frac{g^2}{8} = G_F\frac{M_W^2}{\sqrt{2}}, \tag{88}$$

where G_F is the Fermi constant [4]. Thus, the vacuum expectation value v can be derived directly from the very precise measurement of G_F as

$$v = \left(\sqrt{2}G_F\right)^{-1/2} \approx 246\ \text{GeV}. \tag{89}$$

Considering the diagonal terms of the matter Lagrangian, the neutral gauge boson couplings to leptons are given by:

$$\begin{aligned}\mathcal{L}_{NC} =& \frac{gg'}{\sqrt{g^2+g'^2}}\bar e\gamma^\mu e A_\mu - \frac{\sqrt{g^2+g'^2}}{2}\bar\nu_L\gamma^\mu\nu_L Z_\mu \\ &+ \frac{1}{\sqrt{g^2+g'^2}}\left[-g'^2\,\bar e_R\gamma^\mu e_R + \frac{g^2-g'^2}{2}\bar e_L\gamma^\mu e_L\right]Z_\mu \end{aligned} \tag{90}$$

Therefore, we can identify A_μ as the photon from QED if we require:

$$\frac{gg'}{\sqrt{g^2+g'^2}} = e. \tag{91}$$

Moreover, from the definition of the weak mixing angle θ_W we obtain a relation where the strengths of the weak and electromagnetic interactions are now related through a single parameter:

$$g = \frac{e}{\sin\theta_W} \geq e, \tag{92}$$

$$g' = \frac{e}{\cos\theta_W} \geq e. \tag{93}$$

Rewriting the neutral current Lagrangian in terms of the weak mixing angle:

$$\begin{aligned}\mathcal{L}_{NC} &= e\bar{e}\gamma^{\mu}eA_{\mu} - \frac{g}{2\cos\theta_W}\bar{\nu}_L\gamma^{\mu}\nu_L Z_{\mu} \\ &\quad - \frac{g}{2\cos\theta_W}\left[2\sin^2\theta_W\bar{e}_R\gamma^{\mu}e_R Z_{\mu} + (2\sin^2\theta_W - 1)\bar{e}_L\gamma^{\mu}e_L Z_{\mu}\right] \\ &= e\bar{e}\gamma^{\mu}eA_{\mu} - \frac{1}{\sqrt{2}}\left(\frac{G_F M_Z^2}{\sqrt{2}}\right)^{1/2}\bar{\nu}\gamma^{\mu}(1-\gamma_5)\nu Z_{\mu} \\ &\quad - \frac{1}{\sqrt{2}}\left(\frac{G_F M_Z^2}{\sqrt{2}}\right)^{1/2}\left[2\sin^2\theta_W\bar{e}\gamma^{\mu}(1+\gamma_5)eZ_{\mu} + (2\sin^2\theta_W - 1)\bar{e}\gamma^{\mu}(1-\gamma_5)eZ_{\mu}\right]. \quad (94)\end{aligned}$$

From the two Lagrangians $\mathcal{L}_{CC}$ (87) and $\mathcal{L}_{NC}$ (94), we obtain the lepton interactions with the gauge bosons, which are reported in Figure 5 .

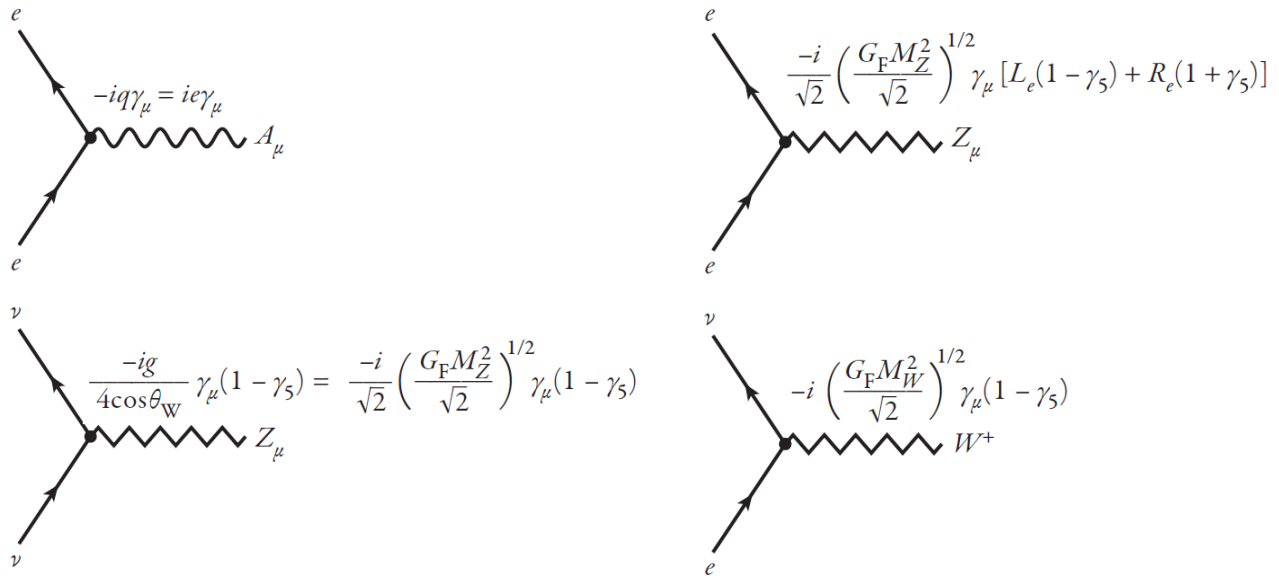

Figure 5: Leptons coupling with the gauge bosons of the $\mathrm{SU(2)_L} \otimes \mathrm{U(1)_Y}$ electroweak theory [1]. For brevity, it is written L_e and R_e, which correspond to $L_e = 2sin^2\theta_W - 1$ and $R_e = 2sin^2\theta_W$.

6 Experimental tests of compatibility of the Higgs couplings with the Standard Model predictions

Having established the theoretical framework of spontaneous symmetry breaking and the Higgs mechanism, we now turn to the experimental tests of the Higgs boson couplings as predicted by the Standard Model. In particular, we consider the 2015 results from the CMS collaboration at the LHC [5]. From proton-proton collisions at LHC, comprehensive sets of production and decay measurements were combined. From the high-resolution $\gamma\gamma$ and ZZ decay channels, the mass of the Higgs boson was determined to be $125.02^{+0.26}_{-0.27}\,(\mathrm{stat})\,^{+0.14}_{-0.15}\,(\mathrm{syst})\,\mathrm{GeV}$, consistent with the expectations from the Standard Model. After the mass determination, the couplings of the Higgs boson were probed for deviations in magnitude from the Standard Model predictions in multiple ways, and no significant deviations were found.

They assumed the signal arises from a single particle with $J^{PC} = 0^{++}$, and a width such that the narrow-width approximation (NWA) holds, permitting its production and decay to be considered independently. In fact, the NWA assumes that the massive state is always produced exactly at its pole as an asymptotic final state. Thus, its decay is an independent

process, expressed by a simple numerical constant known as a branching ratio (BR), which is the fractional probability to decay to a specific final state [6]. Under the assumptions above, the event yield in a given (production)×(decay) mode is related to the production cross section and the decay BR via

$$\sigma(x \to H \to yy) \approx \sigma(x \to H) \times \mathrm{BR}(H \to yy) = \sigma_x \times \frac{\Gamma_{yy}}{\Gamma_{\mathrm{tot}}}, \tag{95}$$

where σ_x is the production cross section through process x, which includes ggH, vector boson fusion (VBF), WH, ZH, and ttH; Γ_{yy} is the partial decay width into the final state yy, such as WW, ZZ, bb, $\tau\tau$, gg, or $\gamma\gamma$; Γ_{tot} is the total width of the boson.

To test the observed data for possible deviations from the rates expected for the SM Higgs boson in the different channels, they introduced coupling modifiers, denoted by the scale factors κ_i. The scale factors were defined for production processes by

$$\kappa_i^2 = \frac{\sigma_i}{\sigma_i^{\mathrm{SM}}}, \tag{96}$$

for decay processes by

$$\kappa_j^2 = \frac{\Gamma_{jj}}{\Gamma_{jj}^{\mathrm{SM}}}, \tag{97}$$

and for the total width by

$$\kappa_H^2 = \frac{\Gamma_{\mathrm{tot}}}{\Gamma_{\mathrm{tot}}^{\mathrm{SM}}}. \tag{98}$$

Thus, the index i can represent many ways to test for deviations from Standard Model, depending on the process taken into account. Moreover, in addition to the κ parameters, the existence of beyond Standard Model (BSM) decays, invisible decays, and undetectable decays of the Higgs boson were considered. The corresponding branching fractions are denoted by BR_{BSM}, BR_{inv} and BR_{undet}. Significant deviations of any κ parameter from unity or of any BR parameter from zero would imply new physics beyond the SM Higgs boson hypothesis.

Now, let us consider four tests that were carried out in the experiment. In Sec. 6.1, it is explored whether κ_W and κ_Z (respectively, the parameters for the Higgs coupling with the W and Z bosons) are compatible with each other and can be meaningfully used together as κ_V (where V stands for massive vector bosons). In Sec. 6.2, the test for deviations that would affect the couplings of massive vector bosons and fermions differently is reported. In Sec. 6.3, the scaling factors among different types of fermions, leptons versus quarks and up-type versus down-type are investigated. In Sec. 6.4, the results of a fit for the tree-level coupling scaling factors and the relation between the observations and the corresponding particle mass are shown.

6.1 Relation between the coupling to the W and Z bosons

In this test, they focused on the scaling factors κ_W and κ_Z that modify the couplings of the SM Higgs boson to the W and Z bosons, and performed two different combined analyses to assess the consistency of the ratio $\lambda_{WZ} = k_W/k_Z$ with unity. The dominant production mechanism populating the 0-jet and 1-jet channels of the $H \to WW \to \ell\nu\ell\nu$ analysis and the untagged channels of the $H \to ZZ \to 4\ell$ analysis is ggH. Therefore, the ratio of their event yields becomes largely insensitive to the Higgs boson production model. This makes it possible to extract a nearly model-independent measurement of λ_{WZ}. Thus, they performed a combined analysis of these two channels with two free parameters, κ_Z and λ_{WZ}. The likelihood scan

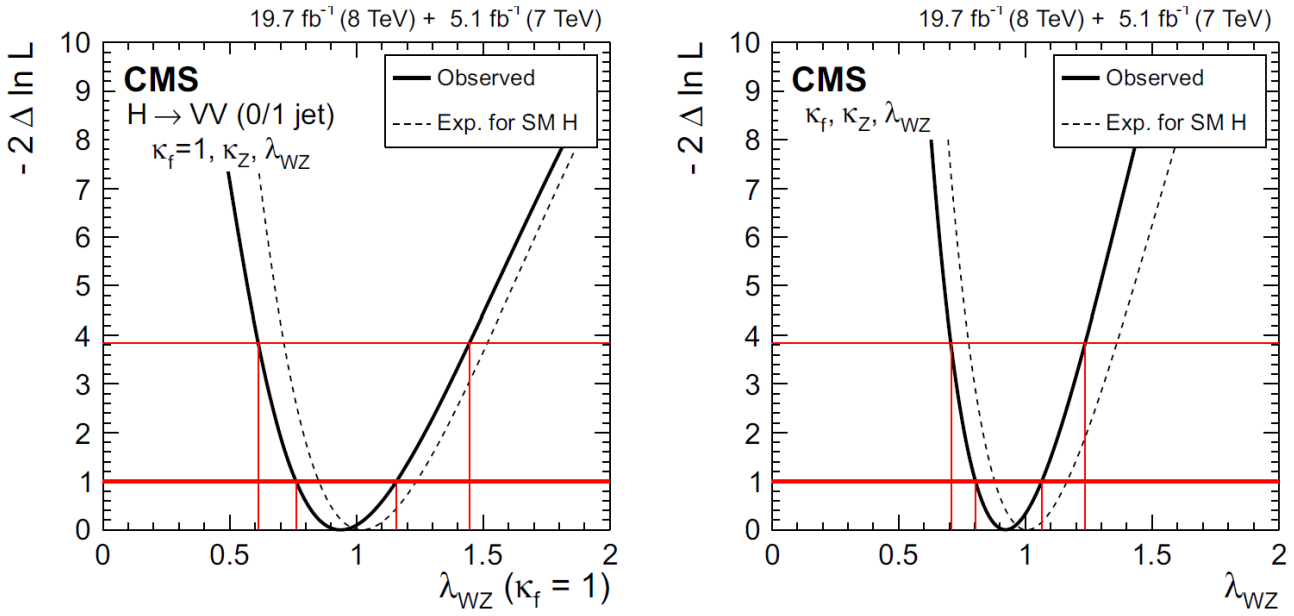

Figure 6: Likelihood scans versus λ_{WZ}, the ratio of the coupling scaling factors to W and Z bosons: (left) from untagged $pp \to H \to WW$ and $pp \to H \to ZZ$ searches, assuming the SM couplings to fermions ($\kappa_f = 1$); (right) from the combination of all channels, profiling the coupling to fermions. The solid curve represents the observation in data. The dashed curve indicates the expected median result in the presence of the SM Higgs boson. Crossings with the horizontal thick and thin lines denote the 68% CL and 95% CL confidence intervals, respectively [5].

versus λ_{WZ} is shown in Figure 6 (left). The scale factor κ_Z is treated as a nuisance parameter. The result of the analysis is

$$\lambda_{WZ} = 0.94^{+0.22}_{-0.18}, \tag{99}$$

which tell us that the data are consistent with the SM expectation ($\lambda_{WZ} = 1$).
They also extracted λ_{WZ} from the combined analysis of all channels. In this approach, they also introduced the parameter κ_f, assuming that the coupling to all fermions is common, but possibly different from the SM expectation. The likelihood scan is shown in Figure 6 (right) with a solid curve. The dashed curve indicates the expected result for the SM Higgs boson, given the current data set. The measured value from the combined analysis of all channels is:

$$\lambda_{WZ} = 0.92^{+0.14}_{-0.12} \tag{100}$$

and is consistent with the expectation from the Standard Model. Thus, it is meaningful to use a common factor κ_V to modify the couplings to W and Z bosons.

6.2 Test of the couplings to massive vector bosons and fermions

As shown in 5.2, the nature of the coupling of the Higgs boson to fermions, through a Yukawa interaction, is different in the SM from the nature of the Higgs boson coupling to the massive vector bosons.
They compared the observations in data with the expectation for the SM Higgs boson by fitting the parameters κ_V and κ_f, assuming $\Gamma_{BSM} = 0$. At leading order, all partial widths scale either as κ_V^2 or κ_f^2, except for $\Gamma_{\gamma\gamma}$, which scales as a function of both κ_V and κ_f. For that reason, the $H \to \gamma\gamma$ channel is the only channel being combined in the analyses that is sensitive to the relative sign of κ_V and κ_f.

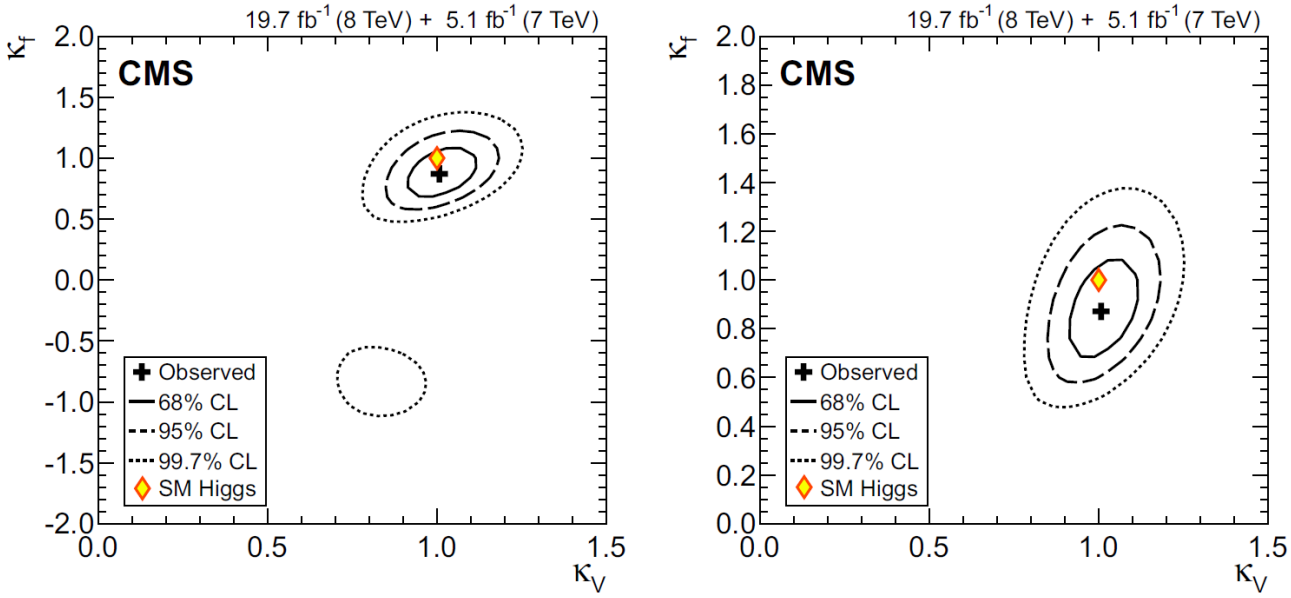

Figure 7: Results of 2D likelihood scans for the κ_V and κ_f parameters. The cross indicates the best-fit values. The solid, dashed, and dotted contours show the 68%, 95%, and 99.7% CL confidence regions, respectively. The diamond shows the SM point $(\kappa_V, \kappa_f) = (1, 1)$. The left plot shows the likelihood scan in two quadrants, $(+, +)$ and $(+, -)$. The right plot shows the likelihood scan constrained to the $(+, +)$ quadrant [5].

Figure 7 shows the 2D likelihood scan over the (κ_V, κ_f) parameter space. While Figure 7 (left) allows for different signs of κ_V and κ_f, Figure 7 (right) constrains the scan to the (+,+) quadrant that contains the SM expectation (1, 1). The 68%, 95%, and 99.7% CL confidence regions for κ_V and κ_f are shown with solid, dashed, and dotted curves, respectively. The data are compatible with the expectation for the Standard Model Higgs boson: the point $(\kappa_V, \kappa_f) = (1, 1)$ lies within the 68% CL confidence region defined by the data. Because of the way these compatibility tests are constructed, any significant deviations from $(1, 1)$ would not have a straightforward interpretation within the SM and would imply BSM physics.

6.3 Test for asymmetries in the couplings to fermions

In this test, they allowed for different ratios of the couplings to down-type fermions and up-type fermions ($\lambda_{du} = \kappa_d/\kappa_u$), or different ratios of the couplings to leptons and quarks ($\lambda_{\ell q} = \kappa_\ell/\kappa_q$). Figure 8 (left) shows the likelihood scan versus λ_{du}, with κ_V and κ_u profiled together with all other nuisance parameters. Figure 8 (right) shows the likelihood scan versus $\lambda_{\ell q}$, with κ_V and κ_q profiled. Assuming that both λ_{du} and $\lambda_{\ell q}$ are positive, the 95% CL confidence intervals are found to be

$$\lambda_{du} \in [0.65,\ 1.39], \qquad \lambda_{\ell q} \in [0.62,\ 1.50]. \tag{101}$$

Thus, there is no evidence that different classes of fermions have different scaling factors.

6.4 Test of the scaling of couplings with the masses of SM particles

Under the assumption that there are no interactions of the Higgs boson other than to the massive SM particles, the data allow a fit for deviations in κ_W, κ_Z, κ_b, κ_τ, κ_t, and κ_μ. In this fit, the loop-induced processes (σ_{ggH}, Γ_{gg}, and $\Gamma_{\gamma\gamma}$) are expressed in terms of the above tree-level κ parameters. The result for this fit is displayed in Figure 9 (left) and shows no significant deviations from the SM expectation.

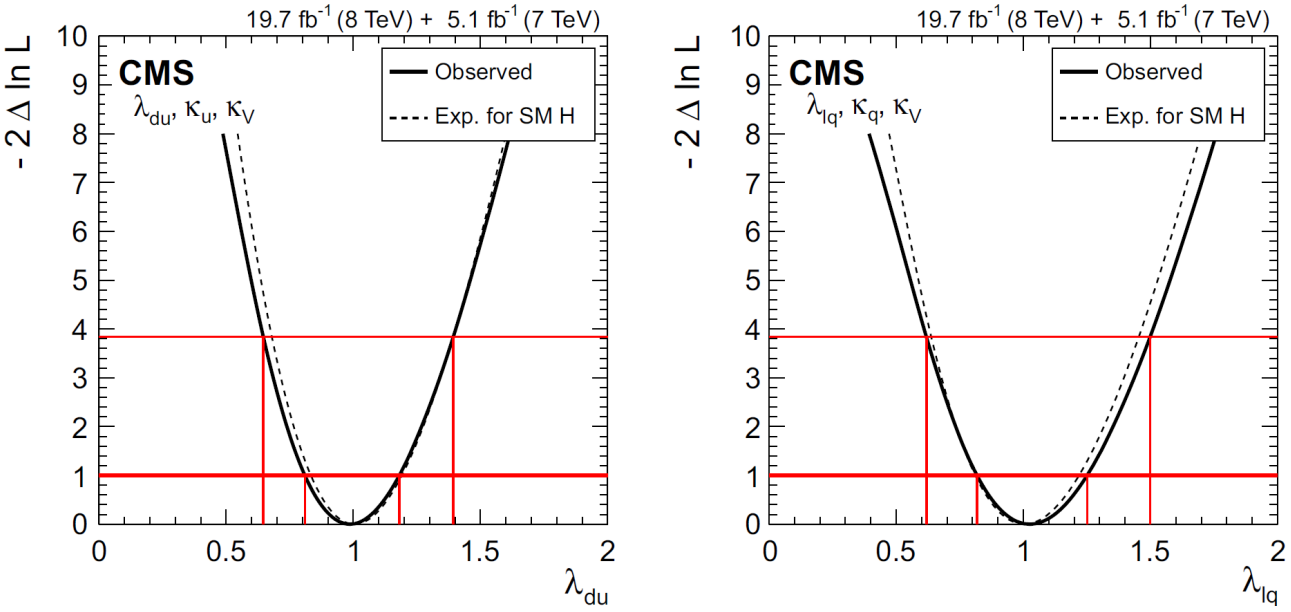

Figure 8: (Left) Likelihood scan versus the ratio of couplings to down-type and up-type fermions, λ_{du}, with the two other free coupling modifiers, κ_V and κ_u, profiled together with all other nuisance parameters. (Right) Likelihood scan versus the ratio of couplings to leptons and quarks, $\lambda_{\ell q}$, with the two other free coupling modifiers, κ_V and κ_q, profiled together with all other nuisance parameters [5].

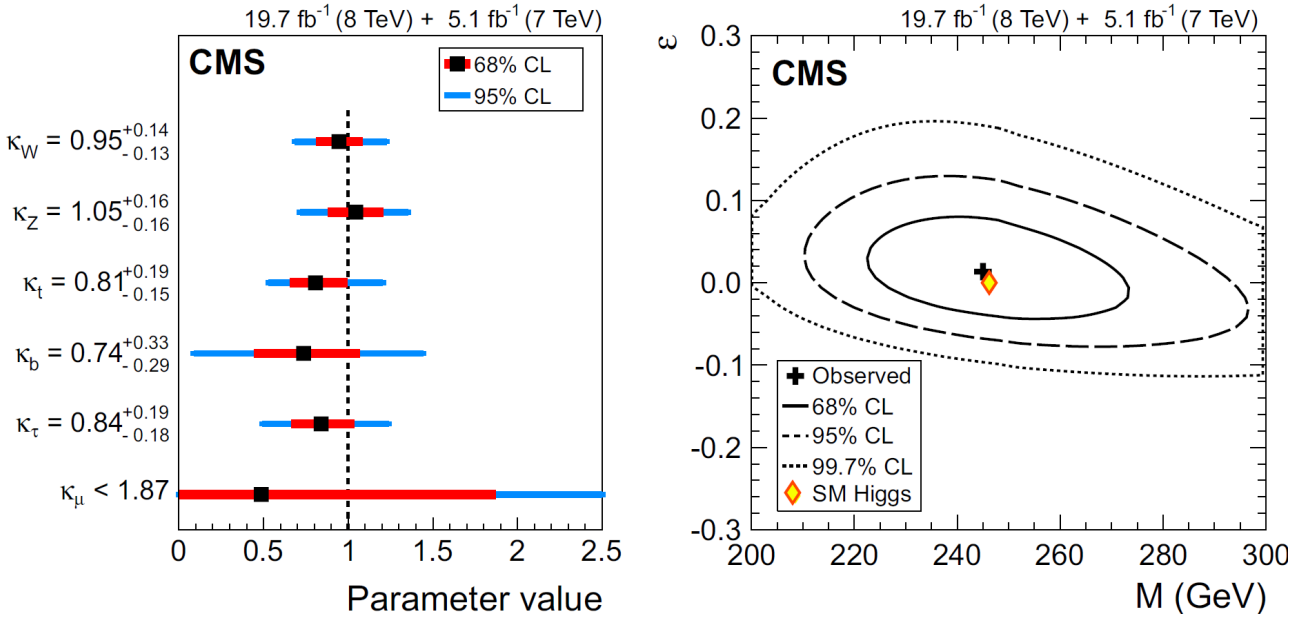

Figure 9: (Left) Results of likelihood scans for a model where the gluon and photon loop-induced interactions with the Higgs boson are resolved in terms of the couplings of other SM particles. The inner bars represent the 68% CL confidence intervals, while the outer bars represent the 95% CL confidence intervals. When performing the scan for one parameter, the other parameters in the model are profiled. (Right) The 2D likelihood scan for the M and ϵ parameters. The cross indicates the best-fit values. The solid, dashed, and dotted contours show the 68%, 95%, and 99.7% CL confidence regions, respectively. The diamond represents the SM expectation, $(M, \epsilon) = (v, 0)$, where v is the SM vacuum expectation value, $v = 246.22$ GeV [5].

As shown in Sec. 5.2.2, the Yukawa coupling between the Higgs boson and the fermions,

λ_f, is proportional to the mass of the fermion, m_f, through the relation $m_f = \lambda_f v/\sqrt{2}$. On the contrary, the coupling to weak bosons, g_V, involves the square of the mass of the weak boson, m_V (see Sec. 5.2.1). Considering these differences, they introduced a parameterization relating the masses of the fermions and weak bosons to the corresponding κ modifiers using two parameters, M and ϵ. In such a model, one has for each fermion $\kappa_f = v\, m_f^{\epsilon}/M^{1+\epsilon}$, and for each weak boson $\kappa_V = v\, m_V^{2\epsilon}/M^{1+2\epsilon}$, where v is the vacuum expectation value, $v = 246.22$ GeV (see Sec. 5.2.2). The SM expectation, $\kappa_i = 1$, is recovered when $(M, \epsilon) = (v, 0)$.
The likelihood scan for (M, ϵ) is shown in Figure 9 (right). It can be seen that the data do not significantly deviate from the SM expectation. The 95% CL confidence intervals for the M and ϵ parameters are

$$M \in [217,\ 279]\ \text{GeV}, \qquad \epsilon \in [-0.054,\ 0.100]. \tag{102}$$

The results of the two fits above are plotted versus the particle masses in Figure 10. Since $g_V \sim \kappa_V 2m_V^2/v$ and $\lambda_f \sim \kappa_f m_f/v$, they chose to plot a "reduced" weak boson coupling, $\sqrt{g_V/(2v)} = \kappa_V^{1/2} m_V/v$. This choice allows fermion and weak boson results to be plotted together.
It is possible to observe that the scaling factor for the coupling of the boson with muons is clearly imprecise. However, the picture that arises from covering more than three orders of magnitude in particle mass is that the boson couples differently to the different particles and that those couplings are related to the mass of each particle.

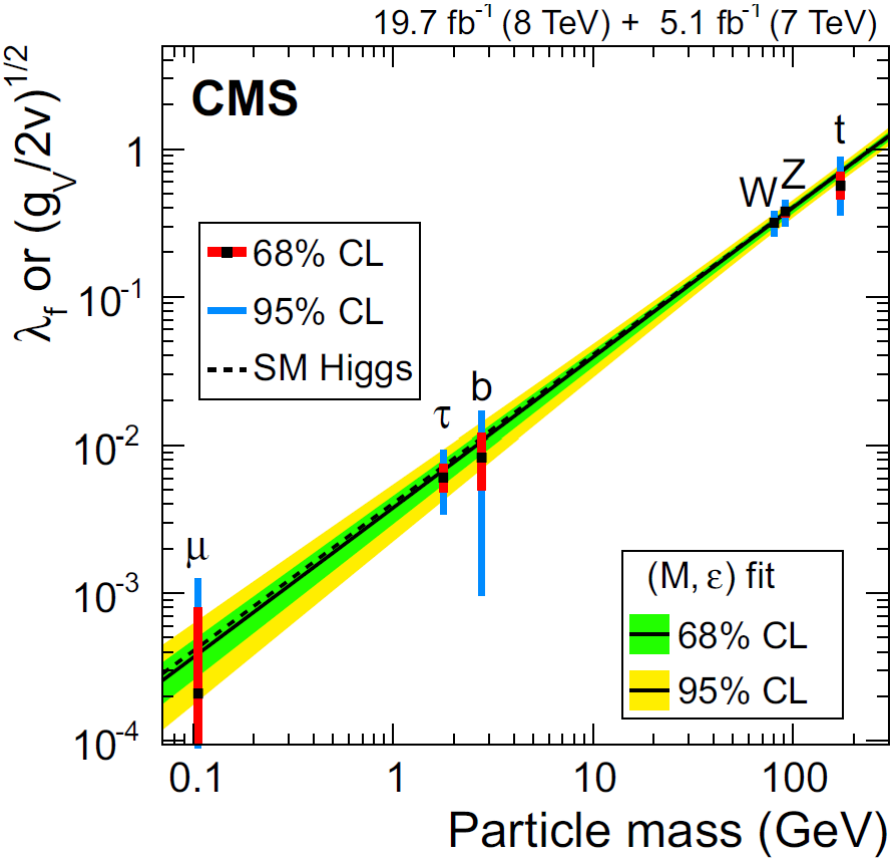

Figure 10: Graphical representation of the results obtained for the models considered in Figure 9. The dashed line corresponds to the SM expectation. The ordinates are different for fermions and massive vector bosons to take into account the expected SM scaling of the coupling with mass, depending on the type of particle. The result of the (M, ϵ) fit from Figure 9 (right) is shown as the continuous line, while the inner and outer bands represent the 68% and 95% CL confidence regions.

References

[1] Chris Quigg. *Gauge Theories of the Strong, Weak, and Electromagnetic Interactions*. 2nd ed. Princeton and Oxford: Princeton University Press, 2013. ISBN: 978-0-691-13548-9.

[2] Fabio Maltoni. *Theory of the Standard Model - Lecture 06*. Course notes, University of Bologna. 2025. URL: https://virtuale.unibo.it/pluginfile.php/2512415/mod_resource/content/8/Lecture%2006.pdf.

[3] Antonio Pich. "The Standard Model of Electroweak Interactions". In: (Feb. 2005). DOI: 10.48550/arXiv.hep-ph/0502010.

[4] Silvia Arcelli. *Spontaneous Symmetry Breaking and The Higgs Mechanism - Lecture 16*. Course notes, University of Bologna. 2025. URL: https://virtuale.unibo.it/pluginfile.php/2492675/mod_resource/content/32/SP-Lecture16.pdf.

[5] V. Khachatryan et al. "Precise determination of the mass of the Higgs boson and tests of compatibility of its couplings with the standard model predictions using proton collisions at 7 and 8 TeV". In: *The European Physical Journal C* 75.5 (May 2015), p. 212. ISSN: 1434-6052. DOI: 10.1140/epjc/s10052-015-3351-7. URL: https://doi.org/10.1140/epjc/s10052-015-3351-7.

[6] D. Berdine, N. Kauer, and D. Rainwater. "Breakdown of the Narrow Width Approximation for New Physics". en. In: *Physical Review Letters* 99.11 (Sept. 2007). arXiv:hep-ph/0703058, p. 111601. ISSN: 0031-9007, 1079-7114. DOI: 10.1103/PhysRevLett.99.111601. URL: http://arxiv.org/abs/hep-ph/0703058.